Structure, Vol. 12, 1519–1531, August, 2004, ©2004 Elsevier Ltd. All rights reserved. DOI 10.1016/j.str.2004.05.023

A Basis for SUMO Protease Specificity Provided by Analysis of Human Senp2 and a Senp2-SUMO Complex

David Reverter and Christopher D. Lima*
Structural Biology Program
Sloan-Kettering Institute
New York, New York 10021

Summary

Modification of cellular proteins by the ubiquitin-like protein SUMO is essential for nuclear metabolism and cell cycle progression in yeast. X-ray structures of the human Senp2 catalytic protease domain and of a covalent thiohemiacetal transition-state complex obtained between the Senp2 catalytic domain and SUMO-1 revealed details of the respective protease and substrate surfaces utilized in interactions between these two proteins. Comparative biochemical and structural analysis between Senp2 and the yeast SUMO protease Ulp1 revealed differential abilities to process SUMO-1, SUMO-2, and SUMO-3 in maturation and deconjugation reactions. Further biochemical characterization of the three SUMO isoforms into which an additional Gly-Gly di-peptide was inserted, or whereby the respective SUMO tails from the three isoforms were swapped, suggests a strict dependence for SUMO isopeptidase activity on residues C-terminal to the conserved Gly-Gly motif and preferred cleavage site for SUMO proteases.

Introduction

Ubiquitin and ubiquitin-like proteins contribute to regulation of cellular pathways involved in apoptosis, differentiation, development, responses to stress, and the cell cycle. Ubiquitin and ubiquitin-like family members are 8–11 kDa proteins that are observed conjugated to target proteins via an isopeptide bond between ubiquitin and a lysine of the protein target (Hershko and Ciechanover, 1998; Hochstrasser, 1998; Laney and Hochstrasser, 1999; Saitoh et al., 1997). The SUMO protein family belongs to a group of ubiquitin-like modifiers that is observed in organisms ranging from yeast to human. The budding yeast *Saccharomyces cerevisiae* contains one SUMO ortholog named Smt3 (Meluh and Koshland, 1995), and SUMO conjugation in yeast appears critical for septin ring formation, chromosomal segregation, and progression of the cell cycle through G_2-M (Johnson and Blobel, 1999; Takahashi et al., 1999; Tanaka et al., 1999; Li and Hochstrasser, 1999).

Mammals contain at least three SUMO family members, SUMO-1, SUMO-2, and SUMO-3. SUMO-2 and SUMO-3 share only 43% and 42% identity to SUMO-1, respectively, but are highly related and share greater than 96% sequence identity to each other. *S. cerevisiae* Smt3 shares 43% amino acid identity with mammalian SUMO-1, 39% with SUMO-2, and 40% with SUMO-3. Although structurally similar, SUMO-1 shares only 14% sequence identity with ubiquitin (Saitoh et al., 1997; Yeh et al., 2000) (Figure 1). Recent studies showed the total fraction of SUMO-2/3 in the cell to be greater than that observed for SUMO-1 and that the existing nonconjugated pool of SUMO-2/3 can be converted to conjugated high molecular mass proteins upon stress stimuli (Saitoh and Hinchey, 2000). Somewhat analogous to ubiquitin, SUMO-2 and SUMO-3 have been observed to form polymeric chains in vitro; and while SUMO-2 chains have been detected in vivo, their significance remains unclear (Tatham et al., 2001).

SUMO is covalently attached to protein targets through an isopeptide bond that occurs through a lysine ϵ-amino group on the protein target and the SUMO C terminus in a process analogous to that of ubiquitin activation and conjugation (Hershko and Ciechanover, 1998). Prior to activation, SUMO is proteolytically processed from its precursor form to produce a conserved C-terminal Gly-Gly motif (Figure 1). ATP-dependent activation of SUMO is catalyzed in two steps by a SUMO-specific E1 enzyme through adenylation of the C-terminal glycine, and transfer of the adenylate to a conserved E1 cysteine in a reaction that releases AMP and results in an E1-SUMO thioester linkage. The E1-SUMO thioester is then competent for isoenergetic thioester transfer to a cysteine in Ubc9, the SUMO-specific E2 conjugating protein. Although several SUMO-specific E3 cofactors have been identified in recent years, Ubc9 directly interacts with nearly all SUMO targets in vitro through a consensus SUMO motif, thus facilitating direct transfer of SUMO to a lysine ϵ-amino group within the protein target (Bernier-Villamor et al., 2002; Melchior et al., 2003).

SUMO conjugation may be additionally regulated by various E3 cofactors (Melchior et al., 2003), although several observations suggest that levels of SUMO conjugated material can also be regulated by the action of proteases that catalyze SUMO deconjugation (Li and Hochstrasser, 1999, 2000). Functional overlap has been uncovered for the two SUMO deconjugating proteases identified in *S. cerevisiae*, but only Ubl-specific protease 1 or Ulp1 is essential in yeast. Genetic and biochemical analysis suggests that Ulp1 catalyzes two critical functions in the SUMO pathway via an encoded cysteinyl proteinase activity, it processes the Smt3 C-terminal sequence (-GG-ATY) to its mature form (-GG), and it deconjugates Smt3 from the lysine ϵ-amino group of the protein target (Li and Hochstrasser, 1999). Ulp1 has been localized to the nuclear pore complex, and this localization appears critical for its function (Panse et al., 2003). In contrast, Ulp2 is primarily observed in the nucleus, and while Ulp2 is not essential, yeast strains containing the Ulp2 null mutation have profound cellular defects that include a temperature-sensitive growth, abnormal cell morphology, decreased plasmid and chromosome stability, and severe sporulation defects (Li and Hochstrasser, 2000). Most importantly, comparative analysis of Ulp1 and Ulp2 conditional alleles reveal com-

*Correspondence: lima@limalab.org

plex patterns of substrate specificity (Li and Hochstrasser, 2000).

Biochemical and bioinformatic approaches have identified at least seven Ulp1 protease orthologs in human (termed Senp1–3 and Senp5–8) (Yeh et al., 2000; Melchior et al., 2003) (Figure 1). As stated previously, substrate specificity has been observed through analysis of Ulp1/Ulp2 function in yeast, and although preliminary, the greater diversity of human Senp family members suggests that SUMO proteases could play significant roles in regulating levels of SUMO conjugation through localization or specific interaction with SUMO-conjugated proteins. For instance, Senp3 (also known as Smt3IP1) appears proficient in deconjugating SUMO2/3 conjugates, but appears unable to process SUMO precursors to their mature form under similar conditions (Nishida et al., 2000). Senp6 (also known as SUSP1) is localized to the cytoplasm and appears to exhibit specificity toward SUMO-1 (Kim et al., 2000).

The enzymatic properties of Senp2 have also been characterized (Nishida et al., 2001; Zhang et al., 2002), suggesting that this nuclear enzyme is able to deconjugate RanGAP-SUMO-1, -SUMO-2- and -SUMO-3 and is able to hydrolyze all three SUMO precursors in vitro. Senp1 is most similar to Senp2, sharing 57% sequence identity in the catalytic domain. Senp1 is also nuclear and appears capable of cleaving SUMO-1 and SUMO-3 protein conjugates in vivo (Gong et al., 2000). Interestingly, a Senp ortholog was originally identified as a Ulp/Senp family member (termed Senp8), but was later shown to encode deconjugating activity against the small ubiquitin-like modifier Nedd8 (Gan-Erdene et al., 2003; Wu et al., 2003; Mendoza et al., 2003), indicating that Ulp/Senp family members can adapt to interact with proteins other than SUMO.

In several cases, the cellular localization of Senp/Ulp family members has been postulated to play an important role in Senp/Ulp function. Senp2 associates with the nuclear face of the nuclear pore, and restricts Senp2 activity to a subset of the conjugated proteins within the nucleus (Hang and Dasso, 2002; Zhang et al., 2002). Ulp1 appears to be a functional homolog of Senp2 as it is also localized at the nuclear pore complex through interactions between the Ulp1 N-terminal domain and karyopherins that are associated with nucleoporins (Panse et al., 2003). Senp1 has also been shown to be localized to the nucleus (Bailey and O'Hare, 2004), and deletions of the N-terminal domain mislocalize Senp1 and alter the pattern of SUMO conjugates in vivo.

To reveal specific interactions between human SUMO-1 and a Senp family member and to reveal the underlying principles in recognition of sumoylated proteins and the properties of the Senp catalytic domain, we have determined the 2.2 Å resolution X-ray structure of a proteolytically active human Senp2 C-terminal fragment alone and the 2.8 Å resolution X-ray structure of a complex between Senp2 and human SUMO-1. Further biochemical, structural, and sequence analysis reveal aspects of Senp/Ulp protease activities that are responsible for deconjugation and maturation of SUMO-1, SUMO-2 and SUMO-3 isoforms.

Results and Discussion

Structure of Human Senp2 Protease Catalytic Domain Alone and in Complex with SUMO-1

H. sapiens Senp2 is a 589 amino acid protein that contains a C-terminal Ulp-like catalytic domain. Based on our previous structural characterization of Ulp1, a Senp2 fragment that included amino acid residues 364–589 was constructed and expressed in *E. coli* (see Experimental Procedures). For clarity, we will refer to this fragment as Senp2 throughout the remainder of the paper. Our previous studies on the Ulp1 protease were unable to address whether the catalytic domain exists in an active or inactive form prior to interaction with SUMO since the structure of Ulp1 was only solved in the context of the Ulp1-Smt3 complex (Mossessova and Lima, 2000). To gain insights into the activation and specificity determinants of Senp2 in the absence of SUMO-1, the Senp2 catalytic domain was purified to homogeneity, crystallized, and X-ray diffraction data were collected. The Senp2 structure contains two independent molecules in the crystallographic asymmetric unit and was solved by molecular replacement using the Ulp1 catalytic domain as a search model. The model was refined to 2.2 Å with an R factor and R_{free} of 20.2% and 24.3%, respectively (Table 1; see Experimental Procedures). The two independent Senp2 catalytic domains located within the asymmetric unit are similar and can be superimposed within 0.21 Å root-mean-square deviation (rmsd) over 204 Cα atoms.

The complex between Senp2 and SUMO-1 was produced by trapping a chemically stable transition state analog between SUMO-1 and Senp2 using sodium borohydride ($NaBH_4$) to selectively cleave and reduce the deacylation intermediate of the proteolytic reaction (Pickart and Rose, 1986; Mossessova and Lima, 2000). This process results in a covalent thiohemiacetal bond between the Senp2 active site cysteine (Cys548) and the C-terminal SUMO-1 glycine (Gly97; see Experimental Procedures). Diffraction quality crystals were obtained between a 17 amino acid N-terminal deletion of SUMO-1 (SUMO-1[18-97]p and Senp2[364-589]p). The structure of the complex was solved by molecular replacement using the Senp2 catalytic domain, revealing one Senp2-SUMO-1 complex per asymmetric unit. The model for SUMO-1 was manually built using the crystal structure of Smt3 as a starting point. The final model was refined to 2.8 Å with a R factor and R_{free} of 21.4% and 27.5%, respectively (Table 1). Electron density for Senp2 was apparent for a continuous polypeptide chain from Leu366 to Leu589 while electron density for SUMO-1 was observed for a continuous polypeptide chain from Glu20 through to the C-terminal Gly97. As expected, the distance observed between the SUMO-1 Gly97 carbonyl carbon atom and the Senp2 Cys548 sulfur atom suggested the presence of a covalent bond between these two atomic positions.

The Senp2 structure confirms its relationship to the Ulp/Senp protease clan, and analogous secondary structure elements observed in the Ulp1 catalytic domain are also observed in the Senp2 structure (Figure 2A) (Mossessova and Lima, 2000). For clarity, the Senp2

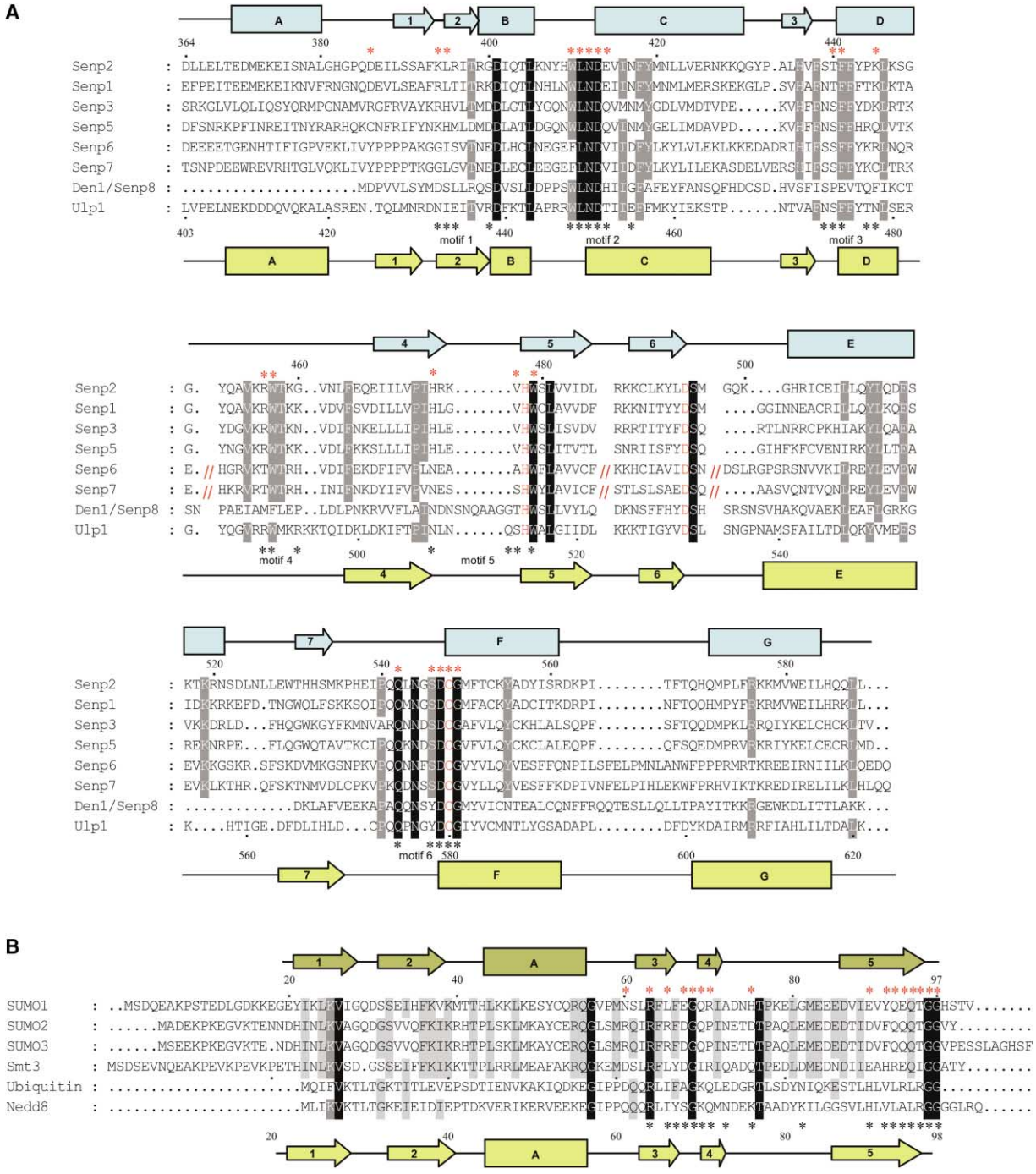

Figure 1. Structure-Based Sequence Alignment of Senp/Ulp1 and SUMO Family Members

(A) Sequence alignment of the catalytic domain of the human Senp family based on structural alignment of human Senp2 and *S. cerevisiae* Ulp1. Gaps are denoted by single dot. Senp2 amino acid numbering shown above the alignment with respect to full-length Senp2 and Ulp1 amino acid numbering shown below alignment with respect to full-length Ulp1. The Senp2 (blue) and Ulp1 (yellow) secondary structural elements are shown above and below the alignment, respectively, with β strands numbered, helices lettered, and coil depicted as a line. Side chain identity is denoted in the alignment with a black background; side chain homology (75% conservation in all sequences) is denoted with a gray background. Conserved catalytic residues in the entire family are shown in red. Red and black asterisks shown above and below the alignment indicate Senp2 or Ulp1 residues in direct contact with either SUMO-1 or Smt3, respectively. Ulp1 motifs 1–6 as described in Mossessova and Lima (2000) are labeled in black below the Ulp1 sequence.

(B) Sequence and structure-based alignment of human SUMO-1 with respect to *S. cerevisiae* Smt3. Sequences of human SUMO-2, SUMO-3, human ubiquitin, and Nedd8 are aligned to human SUMO-1. The SUMO-1 (brown) and Smt3 (yellow) secondary structures are shown above and below the sequence alignment, respectively, with β strands numbered, helices lettered, and coil depicted as a line. Amino acid numbering for human SUMO-1 is shown above the alignment, and amino acid numbering for *S. cerevisiae* Smt3 is shown below the sequence alignment. Red and black asterisks indicate either SUMO-1 or Smt3 residues in direct contact with either Senp2 or Ulp1, respectively.

Table 1. Crystallographic Data

	Senp2	Senp2-SUMO-1
PDB ID	1THO	1TGZ
Source	NSLS X4A	APS 31-ID
Wavelength (Å)	0.9790	0.9790
Resolution limits (Å)	20–2.0	20–2.6
Space group	C2	$P6_522$
Unit cell (Å)	a = 123.24, b = 59.23, c = 94.01; β = 111.29	a = b = 111.63, c = 143.11
Number of observations	258,351	775,500
Number of reflections	36,110	15,675
Completeness (%)	99.1 (99.4)	94.3 (85.4)
Mean I/σI	20.1 (2.6)	10.8 (0.9)
R merge on I[a]	7.3 (48.0)	12.9 (84.1)
Cut-off criteria I/σI	−2	−1
Refinement Statistics		
Resolution limits (Å)	20–2.2	20–2.8
Number of reflections	32,301	13,430
Completeness (%)	99.1	97.0
Cutoff criteria I/σI	0	0
Molecules asymmetric unit	2	1
Residues/atoms	225/1,872 (Senp2)	223/1,861 (Senp2) – 77/610 (SUMO-1)
Number of water atoms	209	81
Number of sulfate atoms		5
R_{cryst}[b]	0.20 (0.29)	0.21 (0.41)
R_{free} (5% of data)	0.24 (0.32)	0.27 (0.39)
Bonds (Å)	0.006	0.007
Angles (°)	1.18	1.32
B factor (mc/sc in Å²)	1.4/2.1	1.2/2.0

Data in parentheses indicate the statistics for date in the highest resolution bin. mc, main chain B factors; sc, side chain B factors.
[a] $R_{merge} = \Sigma hkl\ \Sigma i|I(hkl)i - <I(hkl)>|/\Sigma hkl\Sigma i\ <I(hkl)i>$.
[b] $R_{cryst} = \Sigma hkl\ |Fo(hkl) - F_c(hkl)|/\Sigma hkl\ |F_o(hkl)|$, where F_o and F_c are observed and calculated structure factors, respectively.

structure can be subdivided into two subdomains, an N-terminal segment rich in α helices that contains the protease nucleophile (Cys548; located at the N-terminal end of the central helix αF), and a C-terminal subdomain formed by a central antiparallel five-stranded β sheet surrounded by two α helices. The C-terminal subdomain contains the His478 and Asp495 from the protease catalytic triad located in β5 and β6, respectively.

As was expected, a search of the PDB using DALI (Holm and Sander, 1993) showed that Senp2 shares the highest degree of structural similarity with Ulp1 (1.4 Å rmsd over 210 superimposed Cα atoms with 32% sequence identity). The second top score in the DALI PDB search is to the adenoviral protease-1 fragment (AVP1) with a 3.3 Å rmsd over 136 matching Cα atoms with 16% sequence identity (Ding et al., 1996). The AVP-1 structure represented the prototype of a unique family of cysteine proteases that now includes Ulp1 and other putative desumoylating and deneddylating enzymes. Although AVP1 has been reported to encode deubiquitinating activity (Balakirev et al., 2002), its primary physiological role is believed to involve the processing of viral precursor proteins during virion maturation (Mangel et al., 1993).

The structure determination of the Senp2-SUMO-1 complex reveals the first crystal structure for SUMO-1 (as observed in complex with Senp2) and reveals SUMO-1 secondary structure elements that are conserved throughout the ubiquitin protein family (Figure 2B). Although a 17 amino acid N-terminal deletion for SUMO-1 was utilized in the Senp2-SUMO-1 complex, two additional amino acids (18–19) were disordered and could not be observed. A flexible N-terminal region was also observed for SUMO-1 in the NMR structure and for Smt3 within the context of the Ulp1-Smt3 complex (Bayer et al., 1998; Mossessova and Lima, 2000). Although some differences were observed when comparing the Senp2 structure with the Senp2-SUMO-1 complex, neither Senp2 or SUMO-1 appear to alter their overall topology in response to interaction, indicating that large conformational changes are not required for complex formation (Figure 2).

A PDB search using DALI (Holm and Sander, 1993) and our structure of SUMO-1 showed the highest degree of structural similarity to the crystal structure of yeast Smt3 with an rmsd of 1.4 Å over 77 matching Cα atoms with 48% sequence identity. The second and third highest scores were assigned to ubiquitin (PDB 1UBI, 1.9 Å over 61 matching Cα atoms with 11% sequence identity) and Hub1 (PDB 1M94, 2.2 Å over 60 matching Cα atoms with 10% sequence identity). The fourth and fifth highest scores were assigned to the elonbin b (PDB 1VCB) and a region of the moesin ferm domain (PDB 1EF1). Although identical with respect to sequence, the NMR structure of SUMO-1 was sixth on the scored list with only 63 amino acids aligning to an rmsd of 2.7 Å over 61 matching Cα atoms. While different from the NMR structure, we do not believe SUMO-1 undergoes large conformational changes upon interaction with Senp2. SUMO-1 C-terminal residues remain highly flexible in the SUMO-1

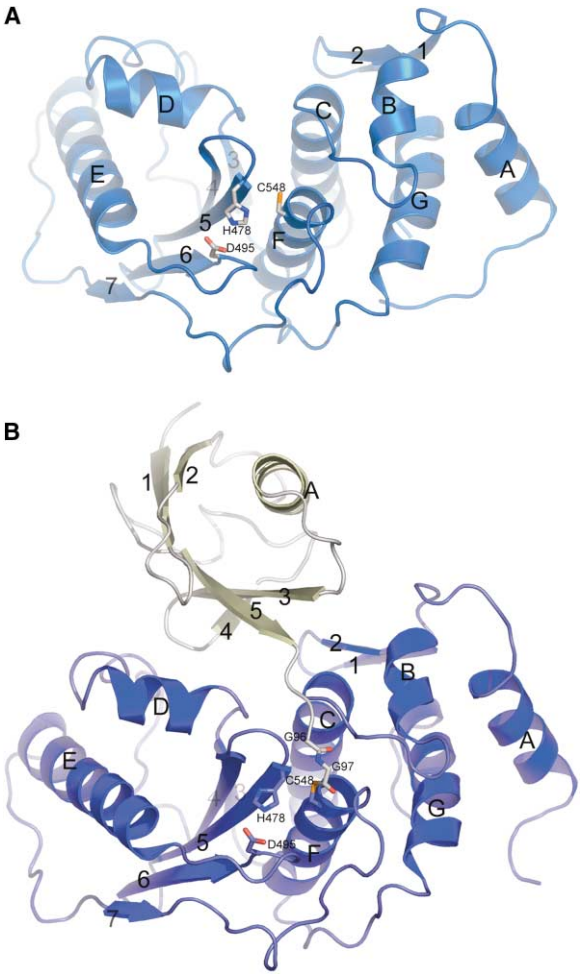

Figure 2. Structure of Senp2 and Senp2-SUMO-1

(A) Ribbon representation of the secondary structure of the human Senp2 catalytic domain. β strands are numbered and α helices are lettered. Catalytic residues are numbered and shown in bond representation.

(B) Ribbon representation of the secondary structure of the human Senp2 catalytic domain (dark blue) in complex with human SUMO-1 (brown). β strands are numbered and α helices are lettered. Senp2 catalytic residues are numbered and shown in bond representation. Graphics prepared using Pymol unless otherwise noted (DeLano, 2002).

NMR structure, but undergo similar rearrangement to that observed in the Ulp1-Smt3 complex by adopting an extended β-like conformation that terminates with a covalent bond between the Gly97 and the catalytic Cys548 in the Senp2-SUMO-1 complex (Figures 2B and 3).

The Senp2 Active Site Alone and in Complex with SUMO-1

The Senp2 active site resembles other cysteine protease active sites and is formed by a catalytic triad of amino acid residues that includes Cys548, His478, and Asp495. Cys548 and His478 are located 3.9 Å from each other on opposite sides of the active site cleft, consistent with traditional roles attributed to these residues for catalytic activity and activation of the cysteine as a nucleophile. Senp2 undergoes local structural rearrangements in response to binding SUMO-1 (Figure 3). His478 undergoes a 180° rotation in the Senp2-SUMO-1 complex such that the imidazole ring now points directly toward Asp495 and away from Cys548. In addition, Trp410 and Trp479 and the imidazole group of His474, residues that interact directly with SUMO-1, all rotate about their Cβ atoms to adapt to interactions with the SUMO-1 C-terminal Gly-Gly motif (Figure 3).

The Senp2 structure can be aligned to Senp2 in complex with SUMO-1 with a 0.41 Å rmsd over 210 Cα atoms. While similar in many respects, some notable differences are observed when the Senp2 structures are aligned based on either the N-terminal (Asp364 to Tyr432 and Pro540 to Leu589) or C-terminal subdomains (Tyr432 to Pro540) (Figure 3). If the N-terminal subdomain is aligned, a significant shift can be observed throughout the C-terminal subdomain that results in ~1.5 Å differences between regions that include αE helix and β7. Deviations appear to originate within the Senp2 C-terminal domain near Pro444 and Pro540, and as depicted in Figure 3, the shift of the C-terminal domain facilitates SUMO-1 interaction insomuch as the substrate binding cleft opens by ~1 Å to enable contacts between the C-terminal residues of SUMO-1 and the Senp2 active site. These interactions include contacts between the conserved SUMO-1 β3-β4 loop (Glu67-Gly68) and side chains of Arg456 and Trp457 of Senp2.

Despite the observed local conformational changes, Senp2 does not appear to be activated by interaction with SUMO insomuch as Senp2 appears catalytically competent in its apo form. This is dissimilar from that observed for HAUSP, a recently characterized member of the UBP family of ubiquitin-specific proteases (Hu et al., 2002). In this structure, the HAUSP catalytic cysteine is misaligned and located 9.7 Å from the catalytic histidine in an inactive state prior to interaction with substrate, in this case, ubiquitin-conjugated P53. Another notable example of protease regulation via active site misalignment was observed in the structure of calpain, a ubiquitous cysteine protease that is active only in the presence of Ca^{2+}. In this case, Ca^{2+} triggers the alignment of the catalytic triad of the active site (Moldoveanu et al., 2002).

Deubiquitinating (DUB) enzymes share no sequence or structural similarity to the Ulp1/Senp protease family, although Ulp and DUB enzymes both belong to a larger group of cysteine proteases that recognize and cleave C-terminal to the conserved C-terminal Gly-Gly motif found in nearly all known ubiquitin or ubiquitin-like proteins (Hochstrasser, 1996; Wilkinson, 1997). The ubiquitin C-terminal hydrolase family (UCH) represents a DUB subfamily that is unable to hydrolyze ubiquitin from large protein conjugates, but is able to catalyze proteolysis of small molecular weight ubiquitin adducts. The crystal structures of a human and a yeast UCH enzyme in complex with ubiquitin aldehyde revealed the mechanism for this selectivity in that recognition of the C-terminal Ub/Ubl Gly-Gly motif was accomplished by a ~21 amino acid crossover loop that folds down on the Ub-aldehyde Gly-Gly motif to provide a steric block to UCH interaction with large ubiquitin adducts (Johnston et al., 1997, 1999).

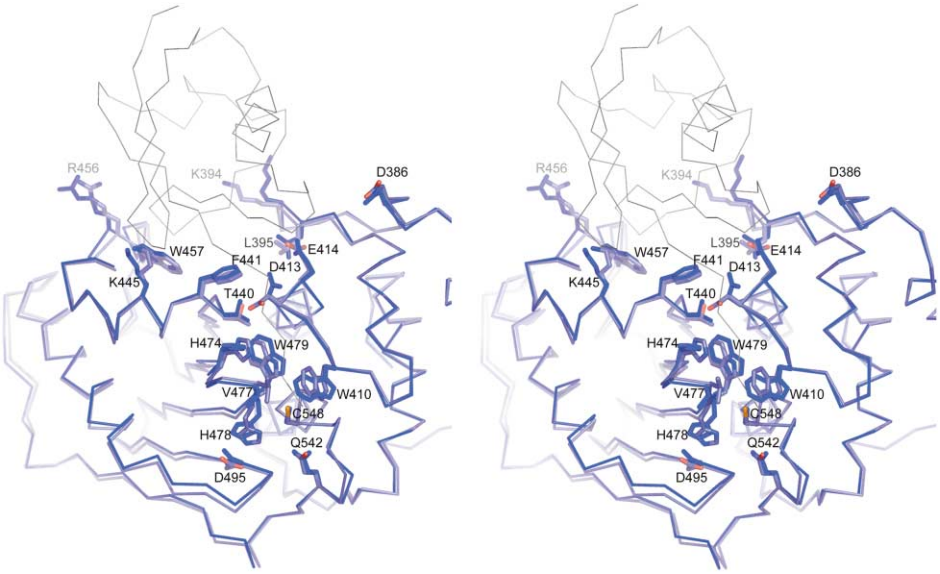

Figure 3. Structural Superposition of Senp2 and the Senp2-SUMO-1 Complex

Stereo representation of Senp2 alone (light blue) and Senp2 (dark blue) in complex with SUMO-1 made by superimposing the respective N-terminal Senp2 subdomains (see text for amino acid numbers). SUMO-1 is represented by a thin gray line. The Senp2 residues involved in interactions with SUMO-1 are labeled and shown in bond representation.

In contrast, Senp2 and Ulp1 can deconjugate large SUMO-protein adducts due to the relatively open configuration of the active site and the lack of an analogous crossover loop as observed in UCH enzymes. As such, Senp2 could allow large protein conjugates to come within a distance suitable for recognition of the isopeptide bond by the active site.

The SUMO-1/Senp2 Interface

SUMO-1-Senp2 interface covers an entire face of the protease, burying 1800 Å^2 of total accessible surface area as calculated with GRASP (Nicholls et al., 1991). Despite sharing only 41% and 29% sequence identity to the yeast counterparts, the SUMO-1 and Senp2 interface can be described in the context of the same six conserved motifs present in the Ulp1-Smt3 structure (Figure 1) (Mossessova and Lima, 2000). Senp2 motifs 1 and 4 form the sides of the interface while the center of the interface is formed by motifs 2, 3, and 5. Motif 6 residues mainly contribute to formation of the Senp2 active site. One portion of the SUMO-1 surface used in Senp2 interaction involves C-terminal SUMO-1 residues Tyr91 to Gly97 (Figure 4A). This region adopts a β strand-like conformation whereby four hydrogen bonds are observed between the backbone of SUMO-1 and residues from motifs 2 and 3 (Asp413, Trp410, His474, and Val477). The extended C-terminal SUMO-1 peptide chain ends with the covalent thiohemiacetal bond between Gly97 and the Sγ atom of Cys548. Gln94 represents the only extensive side chain interaction observed between the SUMO-1 C-terminal peptide and Senp2. Gln94 is within hydrogen bonding distance from Thr440 and is buried in a pocket created by Senp2 residues His474, Trp479, and Phe441.

A major determinant of the SUMO surface recognized by Senp2 includes a conserved salt bridge between Arg63 and Asp413 and the aliphatic side chain atoms from Leu65, Arg63, and Tyr91 that form a complementary hydrophobic pocket that accommodates the Phe441 side chain from Senp2, a residue conserved in all known Senp/Ulp family members (Figure 4B). The significance of these interactions was previously confirmed through a complementary mutational analysis in yeast within the context of the Ulp1-Smt3 complex (Mossessova and Lima, 2000). In that study, mutation of Asp451 (equivalent to Asp413 in Senp2) and Phe474 (Phe441 in Senp2) produced conditional lethality in yeast.

A second major site of interaction between Senp2 and the SUMO-1 C-terminal Gly-Gly motif (Gly96-Gly97 in SUMO-1) occurs near the Senp2 active site. The conformation of the C-terminal tail over the active site suggests that substrates must pass through a constricted hydrophobic tunnel within the active site during cleavage (Figure 4A). This tunnel is mainly formed by Trp410 (motif 2) and Trp479 (motif 5) in interactions with SUMO-1 Gly96 and Gly97, respectively. The orientation of the peptide suggests that binding would be hindered if either position were substituted with any amino acid larger than glycine. The Gly97 carbonyl oxygen is stabilized by interactions with the backbone nitrogen atoms of Cys548, Asp547, and the Nϵ of Gln542 (motif 6). In a true substrate complex, the C-terminal SUMO-1 Gly-Gly motif would either be linked to a lysine side chain from a SUMO-conjugate or to C-terminal amino acid residues within the context of the SUMO maturation reaction.

Functional Characterization of Ulp1/Senp2 Substrate Specificity

As stated previously, three SUMO variants are observed in metazoans, although SUMO-2 and SUMO-3 are highly related to one another in their mature forms (Figure 1). To determine if the catalytic domains from either Senp2

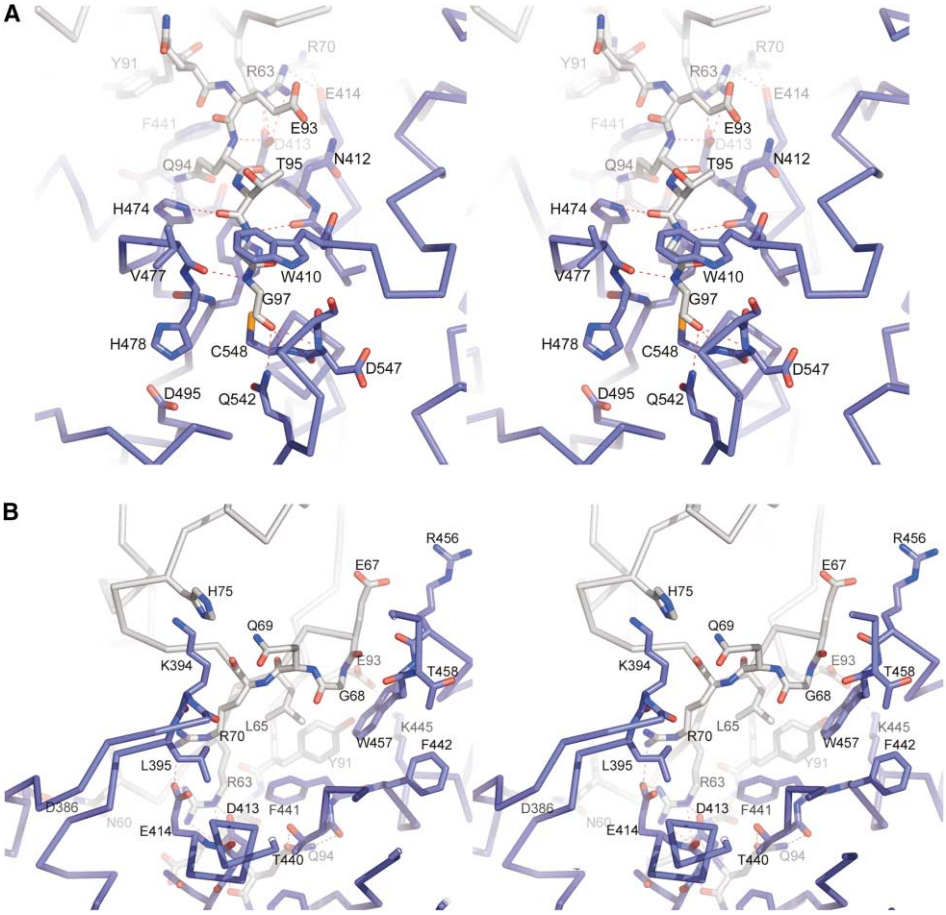

Figure 4. Stereo Representations of the Senp2-SUMO-1 Interface

(A) Stereo representation of the interaction between the SUMO-1 C-terminal tail (gray) and Senp2 (blue). Residues involved in interaction with SUMO-1 are labeled and shown in bond representation. Amino acids thought to participate in hydrogen bonding interactions between these two molecules are denoted by red dashed lines.

(B) Stereo representation focusing on the interactions between SUMO-1 (gray) and Senp2 (blue) that do not involve the Senp2 catalytic residues. Amino acid residues involved in the interaction are labeled and shown in bond representation with hydrogen bonding patterns depicted as red dashed lines.

or Ulp1 can distinguish SUMO-1 from either SUMO-2 or SUMO-3, comparative proteolysis assays were conducted to generate the mature form of these proteins from their respective precursor sequences (Figure 5). Senp2 catalyzes efficient maturation of pre-SUMO-2 when compared to either pre-SUMO-1 or pre-SUMO-3, although all SUMO isoforms can be recognized and cleaved by Senp2 (Figure 5A). Ulp1 catalytic domain was able to efficiently recognize pre-SUMO-1 as a substrate under similar conditions, but was less able to catalyze efficient maturation of pre-SUMO-2 or pre-SUMO-3 (Figure 5B). The SUMO maturation assay utilized 10 nM Ulp1 or Senp2 and 10 μM SUMO-1, -2, or -3. In the Ulp1 reactions, 50% of SUMO-1 was hydrolyzed after 15 min and SUMO-2 and SUMO-3 were not hydrolyzed at appreciable rates compared to SUMO-1. In Senp2 reactions, 50% of SUMO-1, SUMO-2, and SUMO-3 were hydrolyzed after 70, 15, and 160 min, respectively.

The large differences in rates of maturation observed for Senp2 between pre-SUMO-2 and pre-SUMO-3 are surprising since both SUMO-2 and SUMO-3 are nearly identical with the exception of residues C-terminal to the Gly-Gly motif (Figure 1). Furthermore, the inability of Ulp1 to cleave SUMO-2 and SUMO-3 is surprising based on the high level of conservation between Ulp1 and Senp2 within the SUMO binding surface. In addition, most of the critical SUMO residues involved in contacts with either protease are conserved between the various SUMO isoforms. Despite their similarities, some major differences are observed at the respective C-terminal ends of each SUMO isoform. While human SUMO-1 has the C-terminal extension (-GG-HSTV), SUMO-2 has the shortest extension (-GG-VY), and SUMO-3 has the longest extension (-GG-VPESSLAGHSF) (see alignment, Figure 1). To determine if the SUMO tails were responsible for the observed substrate preferences, constructs were assembled to swap each of the respective tails onto each of the SUMO isoforms (Figures 5C and 5D).

SUMO-1 was constructed with the C-terminal tails from SUMO-1, -2, or -3 and so on for both SUMO-2 and SUMO-3 (Figures 5C and 5D). Protease activity assays were conducted under similar conditions to that de-

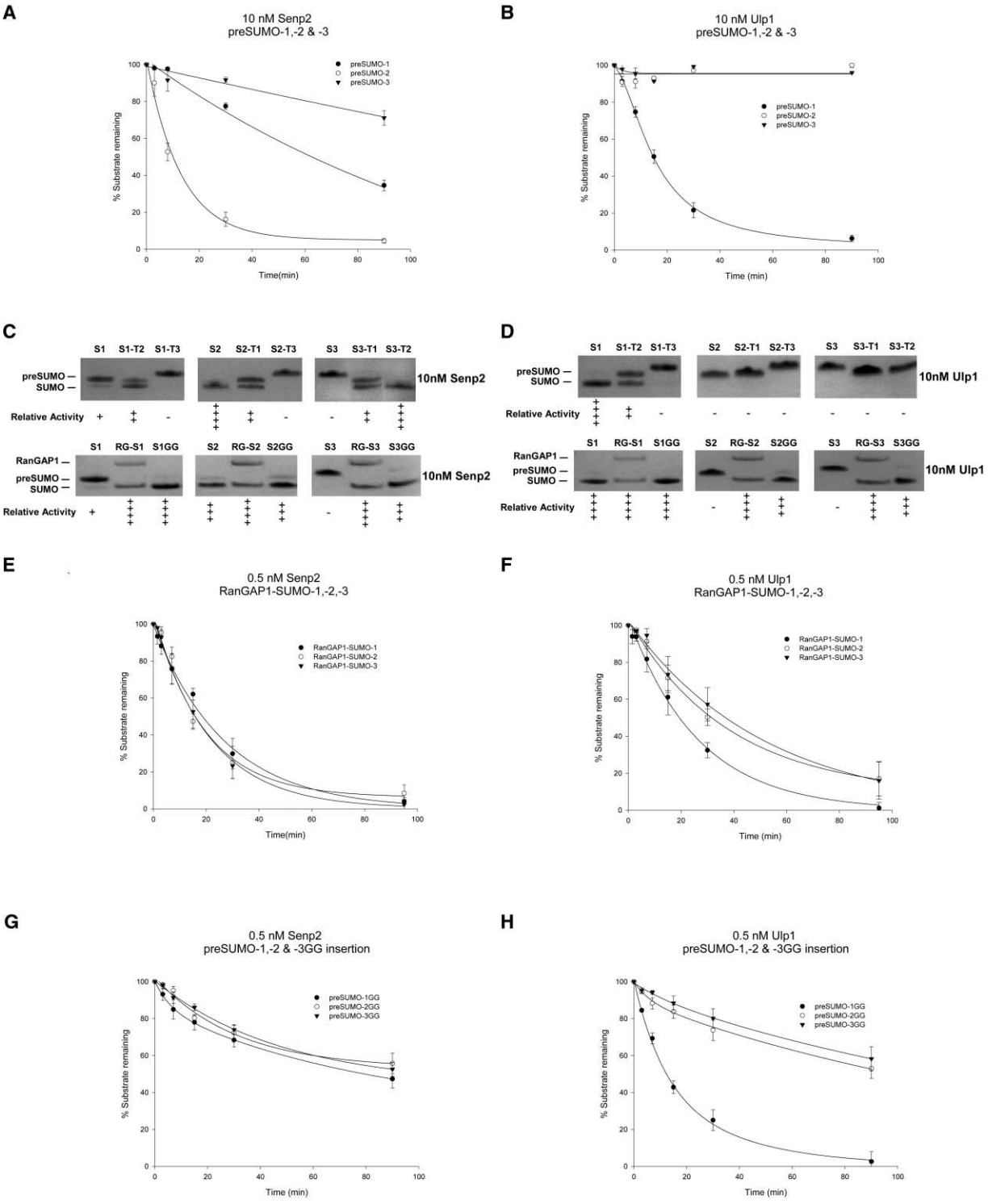

Figure 5. Comparative Proteolysis Assays for SUMO-1, SUMO-2, and SUMO-3 Processing and Deconjugation by Senp2 and Ulp1

(A) Graphical analysis for a time course measuring the maturation reaction for SUMO-1 (closed circle), SUMO-2 (open circle), and SUMO-3 (closed triangle) by human Senp2. The reaction was stopped at different time points by mixing with SDS-PAGE loading buffer. Enzyme and substrate concentration were 10 nM and 10 μM, respectively.

(B) Same reaction as described in (A), but substituting the *S. cerevisiae* Ulp1 catalytic domain for Senp2.

(C) Upper panel, SDS-PAGE gel analysis for the maturation reaction for SUMO-1 (S1), SUMO-1 with C-terminal tail of SUMO-2 (S1-T2), SUMO-1 with C-terminal tail of SUMO-3 (S1-T3), SUMO-2 (S2), SUMO-2 with C-terminal tail of SUMO-1 (S2-T1), SUMO-2 with C-terminal tail of SUMO-3 (S2-T3), SUMO-3 (3), SUMO-3 with C-terminal tail of SUMO-1(S3-T1), and SUMO-3 with C-terminal tail of SUMO-2 (S3-T2) by human Senp2 (10 nM). The reaction was stopped after 30 min by mixing with SDS-PAGE loading buffer. Lower panel, SDS-PAGE analysis for the maturation and deconjugation reaction for SUMO-1 (S1), RanGAP1 conjugated to SUMO-1 (RG-S1), Gly-Gly insertion mutant of SUMO-1 after the natural

scribed for data presented in Figures 5A and 5B, but for single time points at 30 min. Senp2 proteolysis assays of these SUMO hybrids reveals that most of the specificity observed for the native SUMO isoforms can be attributed to the respective SUMO tail (Figure 5C). As stated previously, Senp2 most readily cleaves pre-SUMO-2, but is less able to cleave either pre-SUMO-1 or pre-SUMO-3 by comparison. By placing the SUMO-2 tail on either SUMO-1 or SUMO-3, SUMO-1 and SUMO-3 are now rendered suitable substrates for Senp2. In contrast, Senp2 has the most difficulty processing pre-SUMO-3, and both pre-SUMO-1 and pre-SUMO-2 can be turned into poor substrates by fusing them to the SUMO-3 tail. The data obtained for Ulp1 is as easily interpreted since it is only able to process pre-SUMO-1 with either a SUMO-1 or SUMO-2 tail, but is less able to process any other combination, suggesting that Ulp1 includes elements in its SUMO binding site to permit cleavage of SUMO-1, but not of either SUMO-2 or -3.

Based on the data presented thus far, we sought to further evaluate the importance of amino acid side chains in residues C-terminal to the respective cleavage sites within each SUMO isoform. To test this, Senp2 and Ulp1 catalytic domains were assayed in deconjugation reactions using SUMO-1, -2, and -3 conjugated to the C-terminal domain of RanGAP1 (Figures 5C and 5D, lower panels). In this case, the residue C-terminal to the cleavage site is an aliphatic ϵ-linked lysine side chain. To partially mimic the ϵ-amine linked lysine side chain, an additional Gly-Gly di-peptide was inserted C-terminal to the conserved Gly-Gly motif to generate pre-SUMO-1, -2, and -3 with the C-terminal extensions (-GG-GG-HSTV), (-GG-GG-VY), and (-GG-GG-VPESSLAGHSF), respectively.

Senp2 was able to efficiently hydrolyze SUMO-1, -2, and -3 from RanGAP1, and was able to process the pre-SUMO isoforms containing additional Gly-Gly insertions at nearly equivalent rates, indicating that Senp2 substrate specificity for SUMO-1, -2, or -3 could be attributed to the amino acid side chains C-terminal to the cleavage site (Figure 5C, lower panel). Ulp1 also gained the ability to recognize all three SUMO isoforms that contained the additional Gly-Gly insertion or were conjugated to a lysine within RanGAP1, indicating that the inability of Ulp1 to catalyze proteolysis of SUMO-2 and SUMO-3 in maturation reactions could be attributed to amino acid side chains C-terminal to the cleavage site (Figure 5D, lower panel).

To determine if more subtle preferences for SUMO isoforms still existed, time course assays were conducted using 20-fold less protease than was used to generate Figures 5A–5D. SUMO deconjugation and maturation of SUMO isoforms containing the additional Gly-Gly insertions are presented in Figures 5E–5H. As above, Senp2 loses its ability to discriminate between SUMO-1, -2, and -3 under these conditions, and while Ulp1 gains the ability to interact with all SUMO isoforms in these assays, Ulp1 still retains a slight preference for SUMO-1. In an attempt to reveal the basis for Ulp1 specificity, structure and sequence-based alignments for SUMO and Senp isoforms were again analyzed to identify regions of the Senp-SUMO interface that could account for the remaining differences observed for Ulp1 activity.

SUMO-1 Leu65, Arg70, and His75 are substituted in SUMO-2/3 to arginine, proline, and aspartic acid, respectively (Figures 1, 4B, and 6). Leu65 and Arg70 are conserved in Smt3 while His75 is conservatively substituted to glutamine in Smt3. In the Senp2-SUMO-1 structure, Leu65 appears important for hydrophobic interactions with Phe441, Arg70 interacts directly with Glu414, and His75 is proximal to Lys394 (Figure 6C). Senp2 Phe441, Glu414, and Lys394 all reside within the interface between Senp2-SUMO-1, and substitution at these positions within respective family members might elicit differences in substrate specificity (Figure 6A). Lys394 is conservatively substituted among many of the Senp/Ulp family members, but is substituted to glycine in Senp6 and Senp7, and Asn432 in Ulp1 (Figures 6A and 6C). To test whether Ulp1 Asn432 was important, we mutated Asn432 to lysine to render Ulp1 more similar to Senp2. Proteolysis assays using this mutant Ulp1 isoform revealed no differences in activity, indicating that the subtle preference exhibited by Ulp1 for SUMO-1 could not be explained by analysis of either Ulp1-Smt3 or Senp2-SUMO-1 structures.

Interesting, 20-fold less Ulp or Senp is required to cleave SUMO isoforms from RanGAP, indicating that both proteases interact more readily with SUMO isoforms within the context of a lysine isopeptide linked conjugate. Consistent with this observation, both proteases are more able to interact with and cleave pre-SUMO isoforms that contain an additional Gly-Gly insertion C-terminal to the cleavage site. Past discussion of the structural attributes of the active site observed in both Senp/Ulp-SUMO complexes largely focused on the hydrophobic tunnel through which the conserved SUMO

C-terminal Gly-Gly motif (S1-GG), SUMO-2 (S2), RanGAP1 conjugated to SUMO-2 (RG-S2), Gly-Gly insertion mutant of SUMO-2 after the natural C-terminal Gly-Gly motif (S2-GG), SUMO-3 (S3), RanGAP1 conjugated to SUMO-3 (RG-S3), and Gly-Gly insertion mutant of SUMO-3 after the natural C-terminal Gly-Gly motif (S3-GG) by human Senp2 (10 nM). The reaction was stopped after 30 min by mixing with SDS-PAGE loading buffer. Positive and negative signs underneath panels indicate the relative efficiency of the reaction. Labels for SDS-PAGE gels mark approximate locations of the respective substrates and products of the reactions.

(D) Same reaction as described in (C), but substituting the *S. cerevisiae* Ulp1 catalytic domain for Senp2.

(E) Graphical analysis for a time course measuring the deconjugation reaction for human RanGAP1 conjugated to SUMO-1 (closed circles), SUMO-2 (open circles), and SUMO-3 (closed triangles) by human Senp2. The reaction was stopped at different time points by mixing with SDS-PAGE loading buffer. Enzyme and substrate concentration were 0.5 nM and 3 μM, respectively.

(F) Same reaction as described in (E), but substituting the *S. cerevisiae* Ulp1 catalytic domain for Senp2.

(G) Graphical analysis for a time course measuring the maturation reaction for the C-terminal Gly-Gly insertion mutants of SUMO-1 (closed circles), SUMO-2 (open circles), and SUMO-3 (closed triangles) by human Senp2. The reaction was stopped at different time points by mixing with SDS-PAGE loading buffer. Enzyme and substrate concentration were 0.5 nM and 10 μM, respectively.

(H) Same reaction as described in (G), but substituting the *S. cerevisiae* Ulp1 catalytic domain for Senp2.

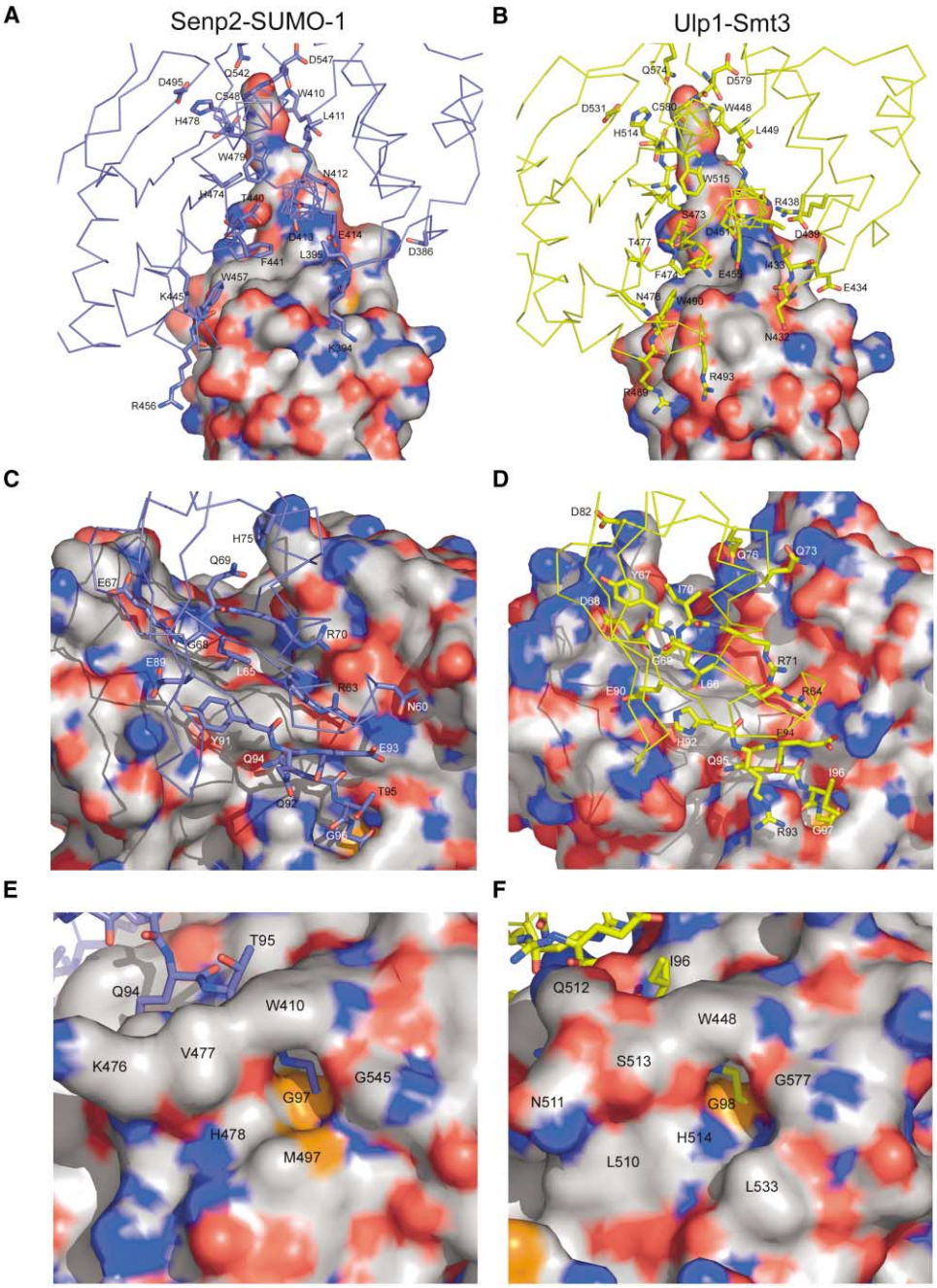

Figure 6. Surface Representation of the Interaction between Senp2-SUMO-1 and Ulp1-Smt3

(A) Surface representation of SUMO-1 in contact with Senp2: surface oxygen atoms are colored red and nitrogen atoms are blue. Senp2 is shown as a thin blue line, labeling and depicting the bond representation of the residues in contact with SUMO-1.

(B) Same orientation as (A), showing the surface representation of the Smt3 in contact with Ulp1. Ulp1 is shown as a thin yellow line, labeling and depicting the bond representation of the residues in contact with Smt3.

(C) Surface representation of human Senp2 interface with SUMO-1. Surface oxygen atoms are colored red and nitrogen atoms are blue. SUMO-1 is shown as a thin blue line, labeling and depicting the bond representation of the residues in contact with Senp2.

(D) Same orientation as (C), but showing the surface representation of Ulp1 in contact with Smt3. Smt3 is shown as a thin yellow line, labeling and depicting the bond representation of the residues in contact with Ulp1.

(E) Same as (C), but rotated to look into the back of the active site where residues C-terminal to the cleavage site in SUMO would be located in a substrate complex.

(F) Same as (E), but viewing the Ulp-Smt3 complex. Protease residues surrounding the active site are labeled on the surfaces of (E) and (F).

Gly-Gly motif must pass. However, substrate preferences C-terminal to the cleavage site suggests that determinants exist within respective catalytic domains that favor interaction with lysine conjugates or substrates that do not include side chains C-terminal to the cleavage site. Inspection of the active sites in Figures 6E and 6F reveal a relatively apolar entrance into the hydrophobic tunnel, including contributions from Trp410, Val477, His478, Met497, and Gly545 in Senp2 and Trp448, Leu510, Ser513, His514, Leu533, and Gly577 in Ulp1. While we are currently unable to attribute specificity for lysine conjugates to any one particular position, the slightly constricted nature of the tunnel combined with its hydrophobic character are both consistent with the observed biochemical data. Although the in vivo relevance of this observation cannot be addressed directly by our biochemical and structural studies, these data suggest that the Senp/Ulp clan of proteases have evolved to maintain their ability to cleave α-peptide linkages while developing the ability to specifically recognize ϵ-linked lysine side chains C-terminal to the cleavage site. However, the apparent lack of substrate specificity toward SUMO conjugates observed for either Senp/Ulp catalytic domains further support the idea that Senp/Ulp SUMO deconjugating activity is regulated through cellular localization in a manner dependent on the more weakly conserved N-terminal domains observed in most Senp family members.

Experimental Procedures

cDNA Cloning and Protein Purification

A human Senp2 cDNA clone was amplified from a human testes cDNA library (Clontech) by PCR, and the sequence was found to be identical to the reported sequence for Senp2 (GenBank number AF151697). An N-terminal His-tagged human Senp2 (364-489)p was expressed from the pET28b in *E. coli* BL21(DE3) codon plus cells (Novagen), purified by Ni-NTA-agarose resin (Qiagen), and dialyzed (25 mM Tris-HCl [pH 8.0], 200 mM NaCl, and 2 mM β-mercaptoethanol) in the presence of thrombin (Sigma). After thrombin cleavage, Senp2 was further purified using a gel filtration Superdex200 column (Amersham-Pharmacia). N-terminally His-tagged SUMO-1 (18-101)p was expressed from pET28b in *E. coli* BL21(DE3) codon plus cells (Novagen), purified by Ni-NTA-agarose resin (Qiagen) and by gel filtration (Superdex75; Amersham-Pharmacia). The covalent adduct was prepared by mixing Senp2 and SUMO-1 at a 1:3 molar ratio with consecutive additions of sodium borohydride ($NaBH_4$) over 30 min to a final concentration of 50 mM to yield 20%–30% of the desired product. The reaction mixture was dialyzed and further purified by cation exchange (MonoS, Pharmacia).

SUMO-2 and SUMO-3 were isolated by PCR from a human testes library (Clontech) and found identical to the reported sequences of SUMO-2 (GenBank number X99584) and SUMO-3 (GenBank number AK024823). Full-length SUMO-1, SUMO-2, and SUMO-3 were expressed from pET28b in *E. coli* BL21(DE3) codon plus cells (Novagen) and purified by excluding the native stop codon and fusing a C-terminal hexa-histidine tag C-terminal to the native polypeptide. SUMO-1, -2, and -3 were purified by Ni-NTA-affinity chromatography (Qiagen) and by anion exchange.

Hybrids of SUMO-1 with the SUMO-2 and -3 tail, SUMO-2 with the SUMO-1 and -3 tail, and SUMO-3 with the SUMO-1 and -2 tail were generated by PCR. Insertion of two additional glycine residues after the native Gly-Gly motif of SUMO-1, -2, and -3 were generated by PCR using the QuikChange Site-Directed Mutagenesis Kit (Stratagene). All mutants were produced in *E.coli* and purified similarly to the native proteins.

Proteolysis Assays

To assay the carboxyl-terminal hydrolase activity, the native SUMO-1, -2, and -3 precursor proteins; the SUMO-1, -2, and -3 C-terminal tail swap mutants; and the SUMO-1, -2, and -3 Gly-Gly C-teminal insertion mutants (10 μM) were incubated with purified Ulp1 or Senp2 (10 or 0.5 nM) at 23°C in buffer containing 25 mM Tris-HCL (pH 8.0), 150 mM NaCl, 0.1% Tween-20, and 2 mM DTT. Time points were taken and the reaction was analyzed by sodium dodecyl sulfate (SDS)-polyacrylamide gel electrophoresis (PAGE) followed by SYPRO staining (Bio-Rad). Protein quantitation was performed using a Gel-Doc apparatus with associated integration software (Quantity-One; Bio-Rad). Processing of SUMO-modified human RanGAP1 was similarly assayed by incubating conjugated NΔ419-RanGAP1-SUMO-1, -2, and -3 (3 μM) with purified Ulp1 or Senp2 (0.5 nM) at 23°C and the reaction was analyzed by SDS-PAGE.

Crystallization and Data Collection

Senp2 crystallization was performed at 4°C using sitting and hanging drop vapor diffusion methods. The reservoir solution contained 20% polyethylene glycol (PEG) 4000, 0.2 M ammonium sulfate, 3% xylitol, and 50 mM sodium citrate, pH 6.25. Single plate-shaped crystals were grown after 3–4 days from equal volumes of protein solution (13 mg/ml in 5 mM Tris, pH 8.0, 25 mM NaCl) and reservoir solution. Prior to diffraction, the crystals were cryo protected in reservoir buffer containing 12% glycerol and flash-frozen in liquid nitrogen. Diffraction data were recorded from 100 K cryocooled crystals at beamline X4A at the National Synchrotron Light Source (Brookhaven, NY). Data were integrated, scaled, and merged using DENZO and SCALEPACK (Otwinowski and Minor, 1997). Senp2 crystals belonged to the monoclinic space group C2 with cell dimensions a = 123.24 Å, b = 59.23 Å, c = 94.02 Å and β = 111.29; and contain two molecules per asymmetric unit (V_M = 3.25 Å^3/Da and 62.21% [v/v] solvent content).

The Senp2-SUMO-1 complex was crystallized at 18°C using sitting and hanging drop vapor diffusion methods. The reservoir solution contained 2 M ammonium sulfate, 5% PEG 400, and 0.1 M bis-tris (pH 6.5). Single hexagonal-shaped crystals were grown after 3–4 days from equal volumes of protein solution (13 mg/ml in 5 mM Tris-HCl, pH 8.0, 25 mM NaCl) and reservoir solution. Prior to diffraction, the crystals were cryo protected in reservoir buffer containing 12% glycerol and flash-frozen in liquid nitrogen. Diffraction data were recorded from 100 K cryocooled crystals at SGX-CAT beam line at the Advanced Photon Source (Argonne, IL). Data were integrated, scaled, and merged using DENZO and SCALEPACK (Otwinowski and Minor, 1997). The Senp2-SUMO-1 crystals belonged to the hexagonal space group $P6_522$ with cell dimensions a = b = 111.16 Å, and c = 143.11 Å; and contain one protein complex per asymmetric unit (V_M = 3.84 Å^3/Da and 68.01% [v/v] solvent content).

Structure Determination and Refinement

The Senp2 structure was solved by molecular replacement using the coordinates of the yeast ortholog Ulp1 as a search model with the program CNS (Brünger et al., 1998). The model was traced manually into the electron density map using the program O (Jones et al., 1991). Refinement was performed with CNS and REFMAC at the last stages (CCP4, 1994). The refined model at 2.2 Å consists of two molecules of 1872 protein atoms and 225 water molecules. All defined amino acid residues exhibit main chain angles falling into the most favored (91.2%) or additionally favored regions (8.4%) of the Ramachandran plot (Laskowski et al., 1993).

The Senp2-SUMO-1 structure was solved by molecular replacement (AMoRe) using the structure of the free Senp2 as a search model (Navaza, 1994). The model was traced manually into the electron density map using the program O. Refinement was performed with CNS and REFMAC at the final stages. The refined model at 2.8 Å consists of one protein complex of 1861 (Senp2) and 610 (SUMO-1) protein atoms and 81 water molecules. All defined amino acid residues exhibit main chain angles falling into the most favored (86%) or additionally favored regions (13.6%) of the Ramachandran plot (Laskowski et al., 1993).

Acknowledgments

We thank the staffs of the SGX-CAT at the Advanced Photon Source and beamline X4A at the National Synchrotron Light Source. Use

of the SGX Collaborative Access Team (SGX-CAT) beamline facilities at Sector 31 of the Advanced Photon Source was provided by Structural GenomiX, Inc., who constructed and operates the facility. D.R. and C.D.L. are supported in part by a grant from the National Institutes of Health (GM65872). D.R. acknowledges support from the Charles H. Revson Foundation, and C.D.L. acknowledges additional support from the Rita Allen Foundation.

Received: March 9, 2004
Revised: May 13, 2004
Accepted: May 27, 2004
Published: August 10, 2004

References

Balakirev, M.Y., Jaquinod, M., Haas, A.L., and Chroboczek, J. (2002). Deubiquitinating function of adenovirus proteinase. J. Virol. *76*, 6323–6331.

Bayer, P., Arndt, A., Metzger, S., Mahajan, R., Melchior, F., Jaenicke, R., and Becker, J. (1998). Structure determination of the small ubiquitin-related modifier SUMO-1. J. Mol. Biol. *280*, 275–286.

Bailey, D., and O'Hare, P. (2004). Characterization of the localization and proteolytic activity of the SUMO-specific protease, SENP1. J. Biol. Chem. *279*, 692–703.

Bernier-Villamor, V., Sampson, D.A., Matunis, M.J., and Lima, C.D. (2002). Structural basis for E2-mediated SUMO conjugation revealed by a complex between ubiquitin-conjugating enzyme Ubc9 and RanGAP1. Cell *108*, 345–356.

Brünger, A.T., Adams, P.D., Clore, G.M., Delano, W.L., Gross, P., Grossekunstleve, R.W., Jiang, J.S., Kuszewski, J., Nilges, M., Pannu, N.S., et al. (1998). Crystallography and NMR system: a new software suite for macromolecular and structure determination. Acta Crystallogr. D. Biol. Crystallogr. *54*, 905–921.

CCP4 (Collaborative Computational Project, Number 4). (1994). The CCP4 suite: programs for protein crystallography. Acta Crystallogr. D Biol. Crystallogr. *50*, 760–763.

DeLano, W.L. (2002). The PyMOL Molecular Graphics System (San Carlos, CA: DeLano Scientific LLC0).

Ding, J., McGrath, W.J., Sweet, R.M., and Mangel, W.F. (1996). Crystal structure of human adenovirus proteinase with its 11 amino acid cofactor. EMBO J. *15*, 1778–1783.

Gan-Erdene, T., Nagamalleswari, K., Yin, L., Wu, K., Pan, Z.Q., and Wilkinson, K.D. (2003). Identification and characterization of DEN1, a deneddylase of the ULP family. J. Biol. Chem. *278*, 28892–28900.

Gong, L., Millas, S., Maul, G., and Yeh, E.T. (2000). Differential regulation of sentrinized proteins by a novel sentrin-specific protease. J. Biol. Chem. *275*, 3355–3359.

Hang, J., and Dasso, M. (2002). Association of the human SUMO-1 protease SENP2 with the nuclear pore. J. Biol. Chem. *277*, 19961–19966.

Hershko, A., and Ciechanover, A. (1998). The ubiquitin system. Annu. Rev. Biochem. *67*, 425–479.

Hochstrasser, M. (1996). Ubiquitin-dependent protein degradation. Annu. Rev. Genet. *30*, 405–443.

Hochstrasser, M. (1998). There's the Rub: a novel ubiquitin-like modification linked to cell cycle regulation. Genes Dev. *12*, 901–907.

Holm, L., and Sander, C. (1993). Protein structure comparison by alignment of distant matrices. J. Mol. Biol. *233*, 123–138.

Hu, M., Li, P., Li, M., Li, W., Yao, T., Wu, J.W., Gu, W., Cohen, R.E., and Shi, Y. (2002). Crystal structure of a UBP-family deubiquitinating enzyme in isolation and in complex with ubiquitin aldehyde. Cell *111*, 1041–1054.

Johnson, E.S., and Blobel, G. (1999). Cell cycle-regulated attachment of the ubiquitin-related protein SUMO to the Yeast Septin. J. Cell Biol. *147*, 981–993.

Johnston, S.C., Larsen, C.N., Cook, W.J., Wilkinson, K.D., and Hill, C.P. (1997). Crystal structure of a deubiquitinating enzyme (human UCH-L3) at 1.8 A resolution. EMBO J. *16*, 3787–3796.

Johnston, S.C., Riddle, S.M., Cohen, R.E., and Hill, C.P. (1999). Structure basis for the specificity of ubiquitin c-terminal hydrolases. EMBO J. *18*, 3877–3887.

Jones, T.A., Zou, J.Y., Cowan, S.W., and Kjeldgaard, M. (1991). Improved methods for building protein models in electron density maps and the location of errors in these models. Acta Crystallogr. A *47*, 110–118.

Kim, K.I., Baek, S.H., Jeon, Y.J., Nishimori, S., Suzuki, T., Uchida, S., Shimbara, N., Saitoh, H., Tanaka, K., and Chung, C.H. (2000). A new SUMO-1-specific protease, SUSP1, that is highly expressed in reproductive organs. J. Biol. Chem. *275*, 14102–14106.

Laney, J.D., and Hochstrasser, M. (1999). Substrate targeting in the ubiquitin system. Cell *97*, 427–430.

Laskowski, R., MacArthur, M., Hutchinson, E., and Thorton, J. (1993). PROCHECK: a program to check the stereochemical quality of protein structures. J. Appl. Crystallogr. *26*, 283–291.

Li, S.-J., and Hochstrasser, M. (1999). A new protease required for cell-cycle progression in yeast. Nature *398*, 246–251.

Li, S.J., and Hochstrasser, M. (2000). The yeast ULP2 (SMT4) gene encodes a novel protease specific for the ubiquitin-like Smt3 protein. Mol. Cell. Biol. *20*, 2367–2377.

Mangel, W.F., McGrath, W.J., Toledo, D.L., and Anderson, C.W. (1993). Viral DNA and a viral peptide can act as cofactors of adenovirus virion proteinase activity. Nature *361*, 274–275.

Melchior, F., Schergaut, M., and Pichler, A. (2003). SUMO: ligases, isopeptidases and nuclear pores. Trends Biochem. Sci. *28*, 612–618.

Meluh, P.B., and Koshland, D. (1995). Evidence that the MIF2 gene of Saccharomyces cerevisiae encodes a centromere protein with homology to the mammalian centromere protein CENP-C. Mol. Biol. Cell *6*, 793–807.

Mendoza, H.M., Shen, L.N., Botting, C., Lewis, A., Chen, J., Ink, B., and Hay, R.T. (2003). NEDP1, a highly conserved cysteine protease that deNEDDylates Cullin. J. Biol. Chem. *278*, 25637–25643.

Moldoveanu, T., Hosfield, C.M., Lim, D., Elce, J.S., Jia, Z., and Davies, P.L. (2002). A Ca(2+) switch aligns the active site of calpain. Cell *108*, 649–660.

Mossessova, E., and Lima, C.D. (2000). Ulp1-SUMO crystal structure and genetic analysis reveal conserved interactions and a regulatory element essential for cell growth in yeast. Mol. Cell *5*, 865–876.

Navaza, J. (1994). An automated package for molecular replacement. Acta Crystallogr. A *50*, 157–163.

Nicholls, A., Sharp, K.A., and Honig, B. (1991). Protein folding and association: insights from the interfacial and thermodynamic properties of hydrocarbons. Proteins *11*, 281–296.

Nishida, T., Tanaka, H., and Yasuda, H. (2000). A novel mammalian Smt3-specific isopeptidase 1 (SMT3IP1) localized in the nucleolus at interphase. Eur. J. Biochem. *267*, 6423–6427.

Nishida, T., Kaneko, F., Kitagawa, M., and Yasuda, H. (2001). Characterization of a novel mammalian SUMO-1/Smt3-specific isopeptidase, a homologue of rat axam, which is an axin-binding protein promoting beta-catenin degradation. J. Biol. Chem. *276*, 39060–39066.

Otwinowski, Z., and Minor, W. (1997). Processing of X-ray diffraction data collected in oscillation mode. Methods Enzymol. *276*, 307–326.

Panse, V.G., Kuster, B., Gerstberger, T., and Hurt, E. (2003). Unconventional tethering of Ulp1 to the transport channel of the nuclear pore complex by karyopherins. Nat. Cell Biol. *5*, 21–27.

Pickart, C.M., and Rose, I.A. (1986). Mechanism of ubiquitin carboxyl-terminal hydrolase. J. Biol. Chem. *261*, 10210–10217.

Saitoh, H., and Hinchey, J. (2000). Functional heterogeneity of small ubiquitin-related modifiers SUMO-1 versus SUMO-2/3. J. Biol. Chem. *275*, 6252–6258.

Saitoh, H., Pu, R.T., and Dasso, M. (1997). SUMO-1: wrestling with a new ubiquitin-related modifier. Trends Biochem. Sci. *22*, 374–376.

Takahashi, Y., Iwase, M., Konishi, M., Tanaka, M., Toh-e, A., and Kikuchi, Y. (1999). Smt3, a SUMO-1 homolog, is conjugated to cdc3, a component of septin rings at the mother-bud neck in budding yeast. Biochem. Biophys. Res. Commun. *259*, 582–587.

Tanaka, K., Nishide, J., Okazaki, K., Kato, H., Niwa, O., Nakagawa,

T., Matsuda, H., Kawamukai, M., and Murakami, Y. (1999). Characterization of a fission yeast SUMO-1 homologue, Pmt3p, required for multiple nuclear events, including the control of telomere length and chromosome segregation. Mol. Cell. Biol. *19*, 8660–8672.

Tatham, M.H., Jaffray, E., Vaughan, O.A., Desterro, J.M., Botting, C.H., Naismith, J.H., and Hay, R.T. (2001). Polymeric chains of SUMO-2 and SUMO-3 are conjugated to protein substrates by SAE1/SAE2 and Ubc9. J. Biol. Chem. *276*, 35368–35374.

Yeh, E.T., Gong, L., and Kamitani, T. (2000). Ubiquitin-like proteins: new wines in new bottles. Gene *248*, 1–14.

Wilkinson, K. (1997). Regulation of ubiquitin-dependent processes by deubiquitinating enzymes. FASEB J. *11*, 1245–1256.

Wu, K., Yamoah, K., Dolios, G., Gan-Erdene, T., Tan, P., Chen, A., Lee, C.G., Wei, N., Wilkinson, K.D., Wang, R., et al. (2003). DEN1 is a dual function protease capable of processing the C terminus of Nedd8 and deconjugating hyper-neddylated CUL1. J. Biol. Chem. *278*, 28882–28891.

Zhang, H., Saitoh, H., and Matunis, M.J. (2002). Enzymes of the SUMO modification pathway localize to filaments of the nuclear pore complex. Mol. Cell. Biol. *22*, 6498–6508.

Accession Numbers

The coordinates for Senp2 and Senp2-SUMO-1 have been deposited in the PDB under ID codes 1THO and 1TGZ, respectively.